Agent-based simulation of city-wide autonomous ride-pooling and the impact on traffic noise

Author(s):
Zwick, Felix; Kuehnel, Nico; Moeckel, Rolf; Axhausen, Kay W.

Publication date:
2021-01

Permanent link:
https://doi.org/10.3929/ethz-b-000454907

Originally published in:
Transportation Research Part D: Transport and Environment 90, https://doi.org/10.1016/j.trd.2020.102673

Transportation Research Part D 90 (2021) 102673

Contents lists available at ScienceDirect

Transportation Research Part D

journal homepage: www.elsevier.com/locate/trd

Agent-based simulation of city-wide autonomous ride-pooling and the impact on traffic noise

Felix Zwick [a,b,*], Nico Kuehnel [c], Rolf Moeckel [c], Kay W. Axhausen [b]

[a] MOIA GmbH, Stadthausbrücke 8, 20355 Hamburg, Germany
[b] Institute for Transport Planning and Systems, ETH Zurich, Stefano-Franscini-Platz 5, 8093 Zurich, Switzerland
[c] Department of Civil, Geo and Environmental Engineering, Technical University of Munich, Arcisstr. 21, 80333 Munich, Germany

ARTICLE INFO

Keywords:
Ride-sharing
Pooled on-demand mobility
MATSim
Traffic noise
Noise model
Shared autonomous vehicles
Emerging mobility

ABSTRACT

Pooled on-demand services promise to provide a convenient mobility experience and increase efficiency of road transport. We apply an established ride-pooling algorithm within the simulation framework MATSim to an autonomous fleet serving almost 2 million requests in Munich. Two mode choice scenarios are implemented, one substituting all car trips by ride-pooling, another one with free mode choice. For both scenarios we compare a stop-based and a door-to-door service in terms of system efficiency and noise imissions, applying an updated noise prediction model in MATSim. The results contribute to the systematic analysis of ride-pooling and show the effects of the proposed policies and service designs, which are essential for an efficient system with low noise exposure. Replacing all car trips by a stop-based ride-pooling system leads to a drastic noise reduction in residential areas whereas door-to-door systems may even increase noise exposure due to additional pick-up/drop-off rides and detours.

1. Introduction

Several app-based dynamic ride-pooling services such as UberPool (2020), GrabShare (2020), CleverShuttle (2020) or MOIA (2020) were introduced in recent years and promise to reduce traffic volumes and resources consumed in urban areas, as several car trips can be bundled and replaced by a single pooled trip. Previous studies have shown the potential of pooled on-demand mobility to reduce traffic and vehicle fleets in urban areas (Martinez and Viegas, 2017; Alonso-Mora et al., 2017) and suggested that ride-pooling can greatly reduce air pollutants and greenhouse gas emissions (GHG) (Greenblatt and Saxena, 2015). However, the positive effects are not only achieved through the introduction of these new services, but must be accompanied by urban policies that make car travel less attractive and prevent a modal shift away from public transport (Naumov et al., 2020).

In contrast to air pollutants and GHG, much less focus has been put on the impact of ride-pooling and shared mobility on traffic noise. Traffic noise is a common nuisance in the urban environment and is largely driven by road traffic. The growth and densification of cities not only leads to higher traffic volumes and noise levels but also to more people being exposed to these levels. According to the WHO, more than 43% of the urban population in Europe is exposed to road noise levels greater than 55 dB(A) (WHO, 2009). Reviews compiled for the WHO indicate that noise can reduce well-being and quality of life of residents, leading to stress and stress-related diseases such as poor mental health (Clark and Paunovic, 2018). In addition, there is a significant relationship between traffic noise levels and the percentage of population that feels highly annoyed (Guski et al., 2017). Noise lowers residential housing

* Corresponding author at: MOIA GmbH, Stadthausbrücke 8, 20355 Hamburg, Germany.
E-mail address: felix.zwick@ivt.baug.ethz.ch (F. Zwick).

https://doi.org/10.1016/j.trd.2020.102673

Available online 26 December 2020

satisfaction and increases chances of people moving away if they can afford it (Bradley and Jonah, 1979; Źróbek et al., 2015; Wardman and Bristow, 2004; Osada et al., 1997), which additionally introduces environmental equity issues. The reduced demand for noisy dwellings has also been found to be reflected in reduced property or rent prices (Kuehnel and Moeckel, 2020).

It has been shown that interventions implemented to reduce noise exposure can be linked to positive health outcomes (Brown and Van Kamp, 2017). It is therefore important to study potential noise reductions of policies such as the implementation of ride-pooling services.

In our study, we introduce an autonomous on-demand ride-pooling service within the simulation framework MATSim (Horni et al., 2016) to the existing transport system in central Munich using a ride-pooling extension by Bischoff et al. (2017). We apply two mode choice scenarios: A draconian one in which the entire car travel demand within the service area is forced to use the new ride-pooling system and a laissez-faire scenario in which all agents are allowed to use the new mode and mode choice decisions are based on an incremental choice model (Koppelman, 1983). For each mode choice scenario, we introduce a door-to-door and a stop-based service and measure system efficiencies, service levels and noise exposure of residential dwellings. In a stop-based service, passengers are picked up and dropped off at predefined stops and need to walk the first and last part of their journey.

The hypotheses are that a) noise exposure should be reduced by replacing conventional car trips with pooled rides and b) residential exposure should decrease even more in a stop-based service than in a door-to-door service and c) service levels (travel time, wait time) are better in the draconian scenario as the service is not affected by congestion caused by individually driven cars.

2. Literature review

The implications that the introduction of a new mobility system has on an existing mobility system are versatile and complex. A common method to assess the system performance, user behaviour, traffic impacts, ecological or economical impacts is to simulate the particular service in a transport model that consists at least of a street network and a population with travel needs. In recent years there have been multiple simulation studies in the field of (pooled) Autonomous Mobility on-Demand (AMoD), often also described as Shared Autonomous Vehicle (SAV) applications.

Pernestål and Kristoffersson (2019) and Jing et al. (2020) reviewed 26 and 44 simulation studies that investigate on the effects of autonomous vehicles, respectively. While each study has a slightly different focus, most focus on driverless taxi applications in urban areas without the capability to pool passengers. Results indicate that the introduction of unpooled fleets causes an increase in vehicle kilometers travelled (VKT) between 5% and 35% compared to the existing system, mainly due to empty kilometers to pick up customers and to reallocate vehicles. At the same time it is stated by Pernestål and Kristoffersson (2019) that in most studies one autonomous vehicle replaces between 6 and 14 conventional cars. If rides are pooled, system efficiency generally increases and VKT can be reduced if penetration rate and request density are large enough. Out of the 44 agent-based simulation studies of autonomous vehicles that Jing et al. (2020) reviewed, almost half (20) made use of the simulation framework MATSim that we also use here. However, there has been extensive investigations in other frameworks that need to be considered. Martinez and Viegas (2017) replaced all private car, bus and taxi trips in Lisbon (approximately 565,000 inhabitants) by a ride-pooling fleet, serving all requests with a maximum time loss of 15 min. They found an overall VKT reduction of 25%, a CO_2 reduction of 32% and that only 4.8% of the city's current car fleet size is necessary to serve the demand.

Alonso-Mora et al. (2017) introduced an anytime optimal ride-pooling algorithm and served all taxi rides (up to 460,700 daily) in Manhattan with a pooled fleet. They found that the vehicle fleet may be drastically reduced from 13,000 single-occupied vehicles to only 3,000 vehicles with a capacity of 4. Service levels are kept at a reasonable level with an average waiting time of less than 3 min and an average trip delay of 3.5 min. Engelhardt et al. (2019) based their investigation of a ride-pooling service on the same algorithm and replaced between 1% and 15% of all car trips in Munich in a similar but slightly larger study area than ours. Their results show that with adoption rates below 5% total VKT increase, whereas higher adoption rates lead to decreased VKT due to pooling. Vehicle flow volumes were mainly reduced on major roads.

Ruch et al. (2020) implemented four previously developed ride-pooling policies (Alonso-Mora et al., 2017; Ma et al., 2013; Fagnant and Kockelman, 2018; Bischoff and Maciejewski, 2016) in the framework AMoDeus (Ruch et al., 2018) that is based on the mobility simulation of MATSim. They applied those four algorithms to an urban scenario with 16,400 requests and a rural scenario with 1,000 requests. Although VKT and fleet sizes can be decreased through pooling compared to an unpooled system, the efficiency gain may not be sufficient to compensate for privacy loss and decreased service levels to attract customers. Pernestål and Kristoffersson (2019) draw the same conclusion from their reviewed papers and propose incentives or public policies to achieve a higher penetration rate of pooled service to accomplish major VKT reductions through on-demand mobility systems.

Bischoff et al. (2017) introduced another ride-pooling extension within MATSim called drt (demand responsive transport) that we also use in this study. They applied a ride-pooling fleet to 27,336 taxi requests that occured on one day in Berlin. It is shown that VKT could be reduced by 15% to 20% compared to the existing taxi system if rides were pooled while average waiting times are below 5 min. High pooling rates occur in the city centre and in the area of the airport where request density is highest.

The drt extension is used in numerous simulation studies (Wang et al., 2018; Vosooghi et al., 2019; Bischoff et al., 2018; Bischoff and Maciejewski, 2020; Leich and Bischoff, 2019). However, all of them consider scenarios on a smaller scale and thus with a lower request density than proposed here.

In general we find that while the impact of ride-pooling on VKT and exhaust emissions has received some attention, the impacts on traffic noise have not yet been investigated systematically.

While car traffic noise depends on the traffic flow volume, the relationship is non-linear and follows a logarithmic curve. In addition, resulting noise *immissions* depend on vehicle speeds, road geometries and the built environment, among others. Therefore,

one cannot infer noise impacts by looking at changes in VKT and traffic volumes alone, which is why the impact of ride-pooling on noise has to be studied explicitly.

A common way of studying noise impacts is to apply noise prediction models (Garg and Maji, 2014; Quartieri et al., 2009). These models take into account traffic volumes and speeds as well as road and building characteristics to estimate emission and immission values. Noise prediction models are an important tool for generating noise maps in compliance with the environmental noise directive 2002/49/EC of the European council (dir, 2002). In Germany, the guideline for noise protection at streets (RLS-19) defines the prediction of road traffic noise (FGSV, 2019). In our study, we make use of this guideline to forecast impacts on noise exposure.

In addition to the introduction of pooled rides, another reduction of noise could be expected from fleets of fully electric vehicles (EV) when compared to internal combustion engine vehicles (ICEV). However, for constant driving speeds above 30 km/h, the main contribution to car traffic noise emerges from the tires rolling on the surface which reduces the potential of reducing noise with EVs (Bekke et al., 2013). Similarly, the European Environmental Agency states that while electric cars contribute to lower noise levels at low speeds, a recent regulation will require the installation of artificial sound generators in all electric and hybrid vehicles by 2021 to improve pedestrian safety, which may further reduce potential reductions in noise (European Environment Agency, 2018). In a recent study, Campello-Vicente et al. (2017) showed that EVs equipped with an acoustic vehicle alerting system still emit lower levels of noise than conventional ICEVs (1 dB(A) less at 30 km/h, compared to EVs without alerting system: 2 dB(A)). The reductions diminish for higher shares of heavy vehicles and lower shares of EVs in the fleet. In the same study, the authors adapted the official French noise prediction model to correct emission values for electric fleets. In a simulation case study in Elche (Spain), they showed that replacing ICEVs with EVs leads to an improvement for 6% to 10% of the local population in terms of noise exposure.

In a state-of-the-art survey by Iversen et al. (2013), the authors presented an overview of studies dealing with possible noise reduction due to EVs. They reported mixed findings, with reductions ranging between 1 and 15 dB(A) at different speeds. Most references indicate that the difference in noise levels vanishes between 30 and 50 km/h. They stressed that these results include a high level of uncertainty and depend on how the comparisons were carried out in detail. Jabben et al. (2012) presented a comparison of noise measurements between ICEVs and EVs in a drive-by scenario and reported reductions between 11 dB(A) at very low speeds and 3 dB(A) at 50 km/h. The same authors implemented a noise prediction model with correction terms for fully electric fleets (Verheijen and Jabben, 2010). The presented correction terms can be distinguished by vehicle types and respective speeds. In an application they found reductions of 3 to 4 dB(A) in noise exposure, on average.

3. Methodology

Travel demand is obtained from the open-source simulation model MITO (Microscopic Transportation Orchestrator, (Moeckel et al., 2020)). MITO is an agent- and trip-based travel demand model that utilizes a modified four step approach to create agent-based trips for six different trip purposes. The program is written in Java. MITO is provided with a synthetic population (Moreno and Moeckel, 2018) and generates trips for individual persons. For each trip, the purpose, destination, mode and time of day are chosen. MITO was estimated with the German national household travel survey (Infas and DLR, 2010) and calibrated to match observed travel behavior.

The simulation is carried out by the Multi-Agent Transport Simulation MATSim (Horni et al., 2016). MATSim is an agent-based transport simulation framework that utilizes an iterative, co-evolutionary learning approach in which each agent tries to maximize their daily score for a given plan of activities. Agents obtain positive scores for performing scheduled activities (such as working) and negative scores for traveling or arriving late at an activity. After every iteration, agents evaluate their last executed plan with a resulting score. While some agents modify their plan by, e.g., choosing a new route or another mode of transport, the remaining agents choose from existing plans based on their scores. In our setup with MITO, we only make use of route choice in MATSim, as mode choice is part of MITO. We only assign car and ride-pooling trips to the network with MATSim. MATSim eventually leads to a stochastic user equilibrium in which no agent can unilaterally increase its perceived score by adapting its plan. Similar to MITO, MATSim is an open-source Java program, which facilitated the integration of the two in one software package.

MATSim contains several extensions to simulate on-demand mobility systems (Maciejewski, 2016). Hörl (2017) developed an extension to simulate (pooled) autonomous taxis, which was further extended by Ruch et al. (Ruch et al., 2018; Ruch et al., 2020) with different operational strategies and algorithms to operate (pooled) autonomous on-demand systems. For this study, we make use of the DRT (demand responsive transit) extension developed by Bischoff et al. (2017). When a trip request with pick-up and drop-off coordinates is submitted, the algorithm searches for a vehicle that can serve the request within a defined maximum wait time and without exceeding a maximum travel time for the waiting customer and all other customers in the vehicle. The performance of the DRT system highly depends on the service parameters, as shown by Bischoff et al. (2017) and Zwick and Axhausen (2020b).

Other pooling strategies, such as the one proposed by Alonso-Mora et al. (2017), collect all requests for a certain time frame and dispatch requests and vehicles after a certain time step, taking into account all requests and vehicles. In this way, the system gains more knowledge of all possible assignments, which may increase the efficiency in high-demand scenarios with limited fleet sizes as shown by Zwick and Axhausen (2020a). The substantially lower computation time in combination with a reasonable system performance led to the decision to apply the algorithm by Bischoff et al. (2017). The DRT extension includes a rebalancing strategy that reallocates idle vehicles to areas with a historically high demand (Bischoff and Maciejewski, 2020). Several studies have shown the beneficial effect of the rebalancing strategy on acceptance rates, travel times and wait times with the potential drawback of increased VKT and consequently more noise exposure (Bischoff and Maciejewski, 2020; Vosooghi et al., 2019; Zwick and Axhausen, 2020a). The algorithm allows to operate a door-to-door service, in which all customers are picked up and dropped off at their desired origin and destination. Alternatively, a stop-based system can be used, in which customers need to walk to and from a pre-defined stop before and after the

ride-pooling trip. The stop-based ride-pooling system promises to decrease noise especially in residential areas without stops as pick-up and drop-off rides in these areas are avoided.

In addition, we make use of MATSim's noise extension by Kaddoura et al. (2017) that is based on an older version of the German guideline for noise protection at streets (FGSV, 1990). In the course of this study, we updated MATSim's extension to work with the more recent version of 2019 (RLS-19) (FGSV, 2019), which updates the estimation procedure of road traffic noise. In addition to the initial noise extension and in line with the RLS, we explicitly account for shielding of buildings (Kuehnel et al., 2019). With the noise extension, we obtain daily averaged noise immission values L_{DEN} (day-evening-night noise level). The estimation takes into account link volumes, vehicle speeds and heavy vehicle shares, among others, to calculate link-level emissions for a given time interval. The L_{DEN} value is a typical indicator for noise exposure at a receiver point and expresses the noise level over an entire day. The aggregated term adds up hourly equivalent noise immission values $L_{\mathrm{eq},k,t}$ at receiver point k at hour t, with an extra penalty τ of 5 dB(A) and 10 dB (A) added to evening (6 pm - 10 pm) and night (10 pm - 6 am) values, respectively:

$$L_{\mathrm{DEN},k} = 10 \cdot \log_{10}\left[\frac{1}{24}\left(\sum_{t=0}^{23} 10^{0.1\cdot(L_{\mathrm{eq},k,t}+\tau(t))}\right)\right], \text{ with} \tag{1}$$

$$\tau(t) = \begin{cases} 0\,\mathrm{dB(A)}, & 6 \leqslant t < 18 \\ 5\,\mathrm{dB(A)}, & 18 \leqslant t \leqslant 22 \\ 10\,\mathrm{dB(A)}, & \text{else.} \end{cases} \tag{2}$$

In contrast to the initial implementation of the RLS-90 guideline, the RLS-19 guideline does not support the "long, straight lane" emission calculation approach anymore. This means that roads (i.e. MATSim links) have to be split in smaller segments such that the length of a segment j_i of a link i is smaller than half of the distance from receiver point k to the midpoint of segment j_i. For this purpose, we implemented an algorithm that recursively splits a link i into smaller segments j_i such that the length condition holds.

The immission values for hour t at receiver point k are calculated as the logarithm of power sums over all emissions $L_{\mathrm{W},j}$ of relevant road segments j_i:

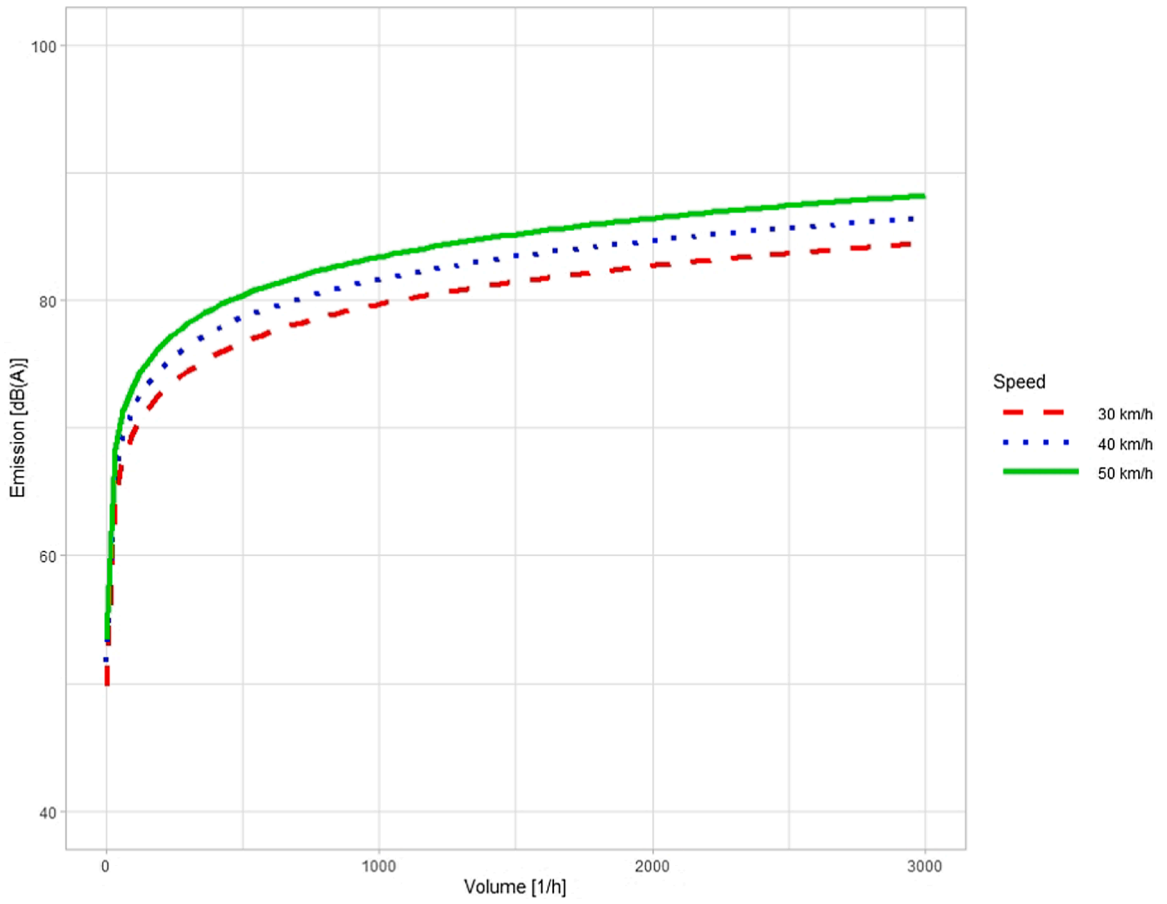

Fig. 1. Dose–response relationship of the uncorrected emission $L_{\mathrm{W},j_i,t}$ for a given link segment dependant on the traffic volume $M_{j_i,t}$ for different speeds $v_{j_i,k,t}$, excluding any correction terms. Based on the RLS-19.

$$L_{\mathrm{eq},k,t} = 10 \cdot \log_{10} \sum_i \sum_{j_i} 10^{0.1 \cdot (L_{\mathrm{W},j_i,t} + 10 \cdot \log_{10}[l_{j_i}] - D_{\mathrm{A},j_i} - D_{\mathrm{RV1},j_i} - D_{\mathrm{RV2},j_i})} \tag{3}$$

where l_{j_i} is the length of segment j_i of link i, D_{A,j_i} is a dampening correction for sound propagation from the link segment, and D_{RV1,j_i} and D_{RV2,j_i} are correction terms for the first and second order reflection, respectively. Due to computational reasons and data availability, the impact of reflections is not taken into account in MATSim's noise model such that reflection correction terms are set to 0. The RLS-19 distinguishes between three different vehicle types k. One type for passenger cars and vans with a weight of up to 3.5 t and two types for heavy-duty vehicles. The ride-pooling vehicles in our study can be seen as passenger vans with a capacity of 6 people with a weight below 3.5 t, and thus, fall into the first category. The emission L_{W,j_i} of a single link segment j_i is calculated as

$$L_{\mathrm{W},j_i,t} = 10 \cdot \log_{10}[M_{j_i,t}] + 10 \cdot \log_{10}\left[\sum_k \lambda_{j_i,k,t} \times \frac{10^{0.1 \cdot L_{\mathrm{W},j_i,k,t}(v_{j_i,k,t})}}{v_{j_i,k,t}}\right] - 30, \tag{4}$$

where M_{j_i} is the average hourly traffic volume, $\lambda_{j_i,k}$ is the share of vehicles of type k, $L_{W,j_i,k}$ is the speed-dependant emission of a vehicle of type k and $v_{j_i,k}$ is the average speed of a vehicle of type k on link segment j_i. The type- and speed-dependant emission is defined as:

$$L_{\mathrm{W},j_i,k,t}(v_{j_i,k,t}) = L_{\mathrm{W0},k,t}(v_{j_i,k,t}) + D_{\mathrm{surf},k}(v_{j_i,k,t}) + D_{\mathrm{grad},k}(g, v_{j_i,k,t}) + D_{\mathrm{inter}}(x_{j_i}) + D_{\mathrm{refl}}(h) \tag{5}$$

Here, $L_{\mathrm{W0},k,t}(v_{j_i,k,t})$ is the base emission value of a vehicle of type k with speed $v_{j_i,k,t}$. $D_{\mathrm{surf},k}(v_{j_i,k,t})$ is a correction for the road surface, $D_{\mathrm{grad},k}(g, v_{j_i,k,t})$ is a correction for the gradient g, $D_{\mathrm{inter}}(x_{j_i})$ is a correction for intersections in a distance of x_{j_i} and $D_{\mathrm{refl}}(h)$ is a correction for multiple reflections for obstacles with a height h. The logarithmic dose–response relationship for a given link is shown in Fig. 1. It becomes obvious that the potential for noise reduction is marginally decreasing with and largely depends on the base traffic volume.

The gradient correction $D_{\mathrm{grad},k}(g, v_{j_i,k,t})$ depends on vehicle type k, speed $v_{j_i,k,t}$ and the gradient g. For the equations for the calculation of the gradient correction we refer to the guideline RLS-19 (FGSV, 2019). The gradient can be obtained by digital elevation models. Another source can be OSM by evaluating the *incline = …* tag. However, this tag is not widely present and sometimes only tagged as *up* or *down* without a percentage.

The surface correction $D_{\mathrm{surf},k}(v_{j_i,k,t})$ is defined for different surfaces and depends on the vehicle type and its speed. Due to lack of surface data, we limit our differentiation of surface types to the surfaces that have a positive correction term (i.e. louder surfaces). These can commonly be obtained by using OSM data. Table 1 shows the link between OSM tags and surface correction terms. The intersection correction $D_{\mathrm{inter}}(x_{j_i})$ is linearly dependent on the distance x_{j_i} from the point source of the link segment j_i to the nearest intersection and is calculated as follows:

$$D_{\mathrm{inter}}(x_{j_i}) = \kappa_\tau * max\left\{1 - \frac{x_{j_i}}{120}; 0\right\} \tag{6}$$

Here, κ_τ is the maximum correction term for the intersection type τ as defined in Table 2. The table also shows the OSM tags that were used to identify the location of intersections during data preparation. In line with uncertain noise benefits of electric vehicles, there is no distinction between the type of engine in the official guideline. However, as discussed above, some reductions in noise could emerge from fully electric fleets. As two of our scenarios assume only electric vehicles on the network, we adapt the calculation of immissions by adding another correction term $D_{\mathrm{electric}}(v_{j_i,k,t})$, similar to the approach of Verheijen and Jabben (2010). For this term, we refer to the reductions presented by Campello-Vicente et al. (2017) and fit an exponentially decreasing function to manually obtained data points from the provided graphs:

$$D_{\mathrm{electric}}(v_{j_i,k,t}) = 5.59 \cdot e^{-0.031 \cdot v_{j_i,k,t}} \tag{7}$$

In line with the RLS-19, the lower bound is set to 30 km/h which is the minimal speed that is assumed for noise estimation. Out of computational reasons and due to lack of data, we ignore the impact of reflections in our approach and set $D_{\mathrm{refl}_{j_i}}(h) \stackrel{\mathrm{def}}{=} 0$. Thus, Eq. (5) becomes:

$$L_{\mathrm{W},j_i,k,t}(v_{j_i,k,t}) = L_{\mathrm{W0},k,t}(v_{j_i,k,t}) + D_{\mathrm{surf},k}(v_{j_i,k,t}) + D_{\mathrm{grad},k}(g, v_{j_i,k,t}) + D_{\mathrm{inter}}(x_{j_i}) + D_{\mathrm{electric}}(v_{j_i,k,t}) \tag{8}$$

MATSim uses a mesoscopic queue-based representation of traffic flow. As such, average speeds and volumes can only be analyzed at the link level. MATSim networks are usually created from OSM ways. In OSM, it is assumed that road surface and gradient stay constant across a way. Therefore, we assume that traffic volumes and speeds, vehicle type shares, velocities, gradient and road surface of each link segment stay constant across the whole link. Applying this assumption to Eq. (3) leads to (see Appendix for the derivation):

Table 1
Surface correction terms for different speeds and surfaces and their respective OSM identifier tags.

Surface type	$D_{\mathrm{surf},k}(v_{j_i,k,t})$ in dB(A) for $v >= \ldots$			OSM tag
	…30 km/h	…40 km/h	…50 km/h	
Cobblestone with smooth surface	1	2	3	'surface = sett'
Other cobblestone	5	6	7	'surface = cobblestone'

Table 2
Maximum correction terms κ_τ and respective OSM identifier tags.

Type τ	Correction κ_τ in dB(A)	OSM Tag
Signalized intersection	3	'highway = traffic_signals'
Roundabout	2	'junction = roundabout'
Other	0	

$$L_{\mathrm{eq},k,t} = 10 \cdot \log_{10}\left[\sum_i \left(10^{0.1 \cdot L_{\mathrm{W},i,t}} \cdot c_i\right)\right], \text{ with} \tag{9}$$

$$c_i = \sum_{j_i} 10^{0.1 \cdot (D_{\mathrm{inter}}(x_{j_i}) + 10 \cdot \log_{10}[l_{j_i}] - D_{\mathrm{A},j_i})} \tag{10}$$

Now only $L_{\mathrm{W},i,t}$ is dependent on t. The corrections for all segments c_i only need to be calculated once and can be stored as a single correction term during a pre-processing step. This means that no matter how detailed links are split, the memory requirement remains the same.

Immissions are calculated for each dwelling of the synthetic population in the service area. This allows us to assess the environmental impact of noise immissions and how it is affected by the introduction of ride-pooling.

4. Data preparation and scenario setup

We apply our simulation setup for the Munich metropolitan area. While our analysis focuses on the core city of Munich, a larger study area was used to generate demand with MITO and MATSim that includes in- and outbound traffic. About 8.8 million daily trips were generated by MITO, out of which 2.9 million travel by car, either as a driver or a passenger. The service area for the new ride-pooling system was defined to cover the service area of the former ride-pooling service CleverShuttle (2020) in Munich shown in Fig. 2.

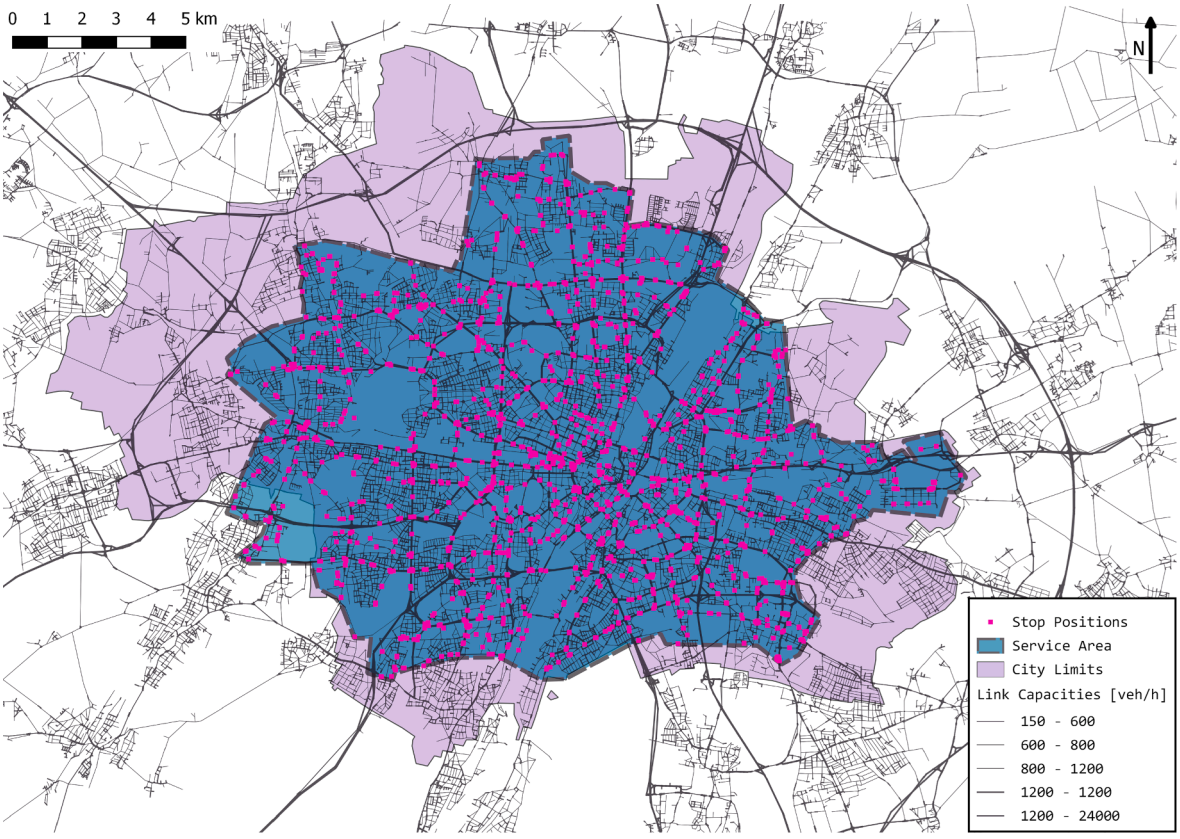

Fig. 2. Service area and (stop) network.

It covers roughly 200 km^2 and contains 1,531 public transport stops, provided by OpenStreetMap (OpenStreetMap Contributors, 2018), which are used for the stop-based service. Previous studies have shown that the stop network design has a major effect on the system efficiency (Zwick and Axhausen, 2020b; Gurumurthy and Kockelman, 2020). In general, a thinner stop network enables more efficient pooling, but customers face longer walking distances. We assume that the public transport stop network is already fairly optimized for the current public transport system. Curb space is already used for pick-up and drop-off areas, which facilitates the usage of those stops for a ride-pooling system. However, additional curb space needs to be created to account for additional vehicles using the stops. For our base case, we simulate all agents of the greater study area that chose to travel by car and measure the resulting VKT and noise exposure within the service area. While it is common to simulate a representative sample of travelers in MATSim to reduce computational runtimes, this is not feasible for the ride-pooling scenarios. Sampling would lead to artifacts in the pooling rate that are difficult to interpret. If a pooled vehicle can carry four passengers and the sampling rate is 10%, it becomes impossible to analyze the occupancy rate due to the discrete number of passengers in agent-based modeling. As the base case serves to define the demand of our first ride-pooling scenario, we also simulate 100% of the car trips.

In both scenarios, we set the maximum wait time to 10 min and the maximum travel time to $1.5\,t_{\text{direct}} + 10\,\text{min}$, where t_{direct} is the direct travel time between the origin and destination. This is assumed to be a reasonable balance between efficiency and a reasonable service level (Zwick and Axhausen, 2020b). If no vehicle can serve a request within the given constraints, the request is rejected and not further considered within the simulation. The stop time for every pick up and drop off is 30 s. The vehicles are assumed to operate 24 h, without accounting for down times for charging, maintenance or other operational issues. For both mode choice scenarios, we operate a door-to-door and a stop-based ride-pooling system, which in combination leads to four different cases that we compare.

To assess noise immissions, we analyze the 647,677 dwellings within the service area (Fig. 2). A receiver point is defined for each dwelling. We do not compute immissions for a regular grid of receiver points as we want to assess exposure of actual residents who do not reside in an even grid with an even density, but in dwellings. Larger buildings may contain multiple apartments. Therefore, the resulting average immission levels will be weighted by household density. In addition to the location of stops, we obtain the positions of tunnels and intersections as well as road surfaces from OpenStreetMap (OpenStreetMap Contributors, 2018). The immission contribution of MATSim links for those tunnels is set to 0. Gradient information is only sparsely available for Munich. However, since Munich is located in the Munich gravel plain, most of the study area is essentially flat. The largest road elevation has a maximum gradient of 4% which would result in a negligible correction term. For our scenario, the gradient correction is therefore set to 0.

We assess two different mode choice scenarios to define the ride-pooling demand. The processes to obtain the demand are described in the following two sections.

4.1. Draconian scenario

In the first mode choice scenario, we assume a radical but simple policy. We replace all existing private car trips that drive in the service area with ride-pooling. We cut out trips that neither start nor end in the service area to reduce the run-time. External-to-internal trips (E-I) and internal-to-external trips (I-E) are transferred to the ride-pooling system within the service area and are assumed to be transported by an alternative mode outside the service area. Travelers using other modes in the base case cannot switch to ride-pooling. This approach is similar to a previous city-wide application of on-demand mobility with unpooled rides by Bischoff and Maciejewski (2016), although they did not replace E-I and I-E car traffic. Through traffic is not taken into account here as the service area does not include the outer motorway ring that is commonly used by trips neither starting nor ending within the service area. We use 18,000 6-seater vehicles for the door-to-door service and 12,000 6-seater vehicles for the stop-based service, which have been identified as sufficient to serve at least 99.8% of all requests.

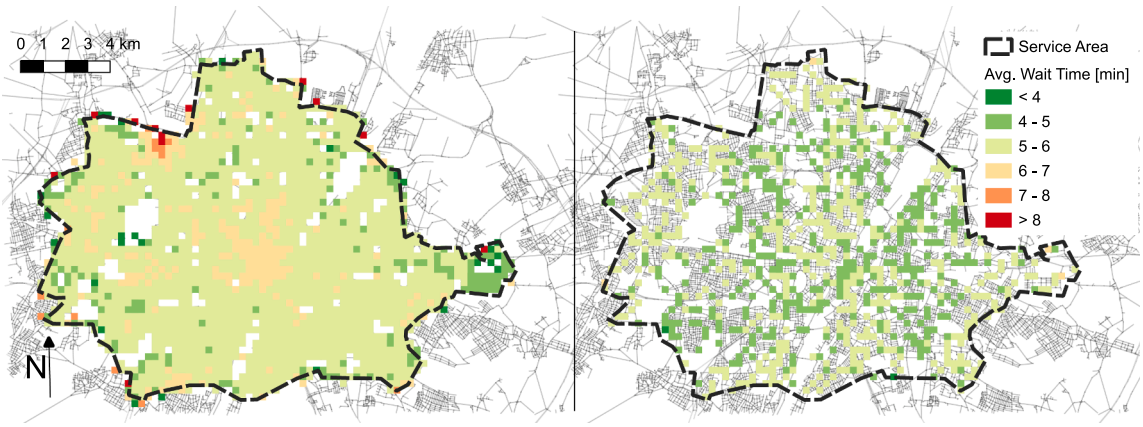

Fig. 3. Average wait times in minutes per zone for the door-to-door (left) and the stop-based (right) service in the draconian scenario.

4.2. Laissez-faire scenario

The second setting applies a laissez-faire scenario in which every agent may choose the new ride-pooling mode. To obtain somewhat realistic mode shares, we add ride-pooling to MITO's mode choice model. Since we have no data to estimate or calibrate the model, we base the agents' decision on an existing utility function and implement the new mode in an incremental logit model (Koppelman, 1983). Due to the absence of a taxi mode in the original model, we assume the mode *car passenger* to be most similar to ride-pooling. Similar to *car passenger*, agents are not driving themselves and do not need a car or a driver's license. While agents use a third-party service and have to share their trip with strangers, which makes it similar to transit modes, we consider the level of comfort to be more similar to a private car. Agents do not have to rely on connections and transfers, there is no predefined schedule and individual seats are guaranteed without the risk of overcrowding. Lastly, even in the stop-based ride-pooling service, routes in general will be more direct than transit routes as any stops can be connected for start and end of a trip. We then re-use the utility coefficients of the *car passenger* mode to calculate utilities for the new mode. The main difference in utility compared to auto passenger are generalized costs. Here, we adjust generalized costs to include wait time, service costs per km and a detour factor for the actual travel time. Since we assume that our service operates autonomously, we obtain a per-kilometer fare from (Bösch et al., 2018) and set it to EUR 0.27. Additionally, a fixed fare of EUR 2 is charged. We use results from a previous draconian scenario to obtain estimates for the average wait times and detour factors. Fig. 3 shows that the average wait times in the draconian scenario are constantly around 5 min for most parts of the service area. Thus, the waiting time for ride-pooling is set to 5 min for all customers. We estimate travel times by using the direct car travel time and multiplying it with an average detour factor taken from a previous simulation. Different from the draconian scenario, we only allow internal-to-internal trips within the service area to be made by ride-pooling. The assumption is that most people would probably not use another mode from/to the boundary of the study area and change from/to ride-pooling if it is not enforced.

We use 8,000 6-seater vehicles for the door-to-door service and 5,000 6-seater vehicles for the stop-based service to serve at least 99.8% of all requests.

5. Results

The presented scenarios are analyzed with regard to system efficiency and traffic noise impact within the service area shown in Fig. 2. After presenting the results of the base case, we compare the system efficiency to the draconian and the laissez-faire scenarios with the two proposed ride-pooling services. Finally, we assess the noise impact in each scenario.

In the base case, overall VKT within the service area is 9.8 million km including the VKT by incoming, outgoing and through traffic. The average travel time for internal trips is 13:01 min for an average trip length of 6.9 km. Consequently, the average travel speed is 32 km/h, which is in line with Forbes (2008) and Engelhardt et al. (2019). Walking to the parked vehicle or parking search traffic are not considered.

5.1. Ride-pooling system performance

The transport system aims at transporting all agents in the shortest possible time to their destination, including short wait and walk times. Table 3 shows performance indicators for the door-to-door ride-pooling service and the stop-based ride-pooling service.

With a door-to-door ride-pooling service, 18,000 vehicles are used to serve almost 2 million rides in the service area that were previously conducted by private vehicles. The VKT of the ride-pooling system are 7.0 million, of which 8% are driven empty to pick up customers and for reallocation purposes. To facilitate the comparison between the scenarios we also measure the VKT inside the service

Table 3
Overview of system performance indicators of the base case system and all ride-pooling (RP) systems within the service area.

	Base case	Draconian scenario		Laissez-faire scenario	
		Door-to-door	Stop-based	Door-to-door	Stop-based
RP vehicles	—	18,000	12,000	8,000	5,000
RP rides	—	1,912,783	1,836,513	503,037	498,529
Rides per RP vehicle	—	106	153	63	100
RP rejections	—	2,926	0	179	132
RP kilometers [km]	—	6.9×10^6	4.5×10^6	1.9×10^6	1.4×10^6
VKT in service area [km]	9.8×10^6	6.6×10^6	4.5×10^6	10.6×10^6	10.1×10^6
Share of empty km [%]	—	8	7	5	6
Avg. travel time [min]	13:01	15:12	14:44	17:01	15:41
Avg. trip length [km]	6.9	9.7	9.6	9.4	9.2
Avg. detour [%]	—	40	41	42	44
Avg. wait time [min]	—	5:30	5:04	5:34	4:56
Median wait time [min]	—	5:37	5:08	5:36	4:43
Avg. walk distance [m]	—	—	271	—	259
Avg. computation time per iteration [h]	1/2	24	16	9	5

Note: Walk distance only includes walk to and from ride-pooling vehicles.

area, which is 6.6 million km in this case. Compared to 9.8 million km in the base case, we observe a substantial reduction with the pooling system. The mean travel time is 15:12 min, the agents face an average detour of 40% and an average wait time of 5:30 min. 2,926 requests (0.15%) could not be served within the maximum wait time of 10 min or the accepted detour parameter.

Using a stop-based ride-pooling service in the draconian scenario, a small part of the requests are not served by the ride-pooling system because origin and destination stops are the same. The remaining 1.8 million requests can be served by only 12,000 vehicles, leading to more than 150 rides per vehicle. The vehicle kilometers driven are further reduced to 4.5 million km, which is a reduction of 54% compared to the base case. The average travel time drops to 14:44 min and the mean wait time to 5:04 min. Additionally, the agents need to walk on average 271 m to and from a stop, or a total of 542 m per trip. None of the requests had to be rejected with the given service constraints.

For the laissez-faire scenarios, MITO's mode choice model predicted a 16% share for autonomous ride-pooling trips starting and ending in the service area. Many of these are home-based, which, including the return trip, translates into two rides per trip. Out of the ride-pooling trips, roughly 47% were previously made by the modes *car* or *car passenger*, 20% by *public transport*, 13% by *bike* and 20% by *walk*. This results in about half a million requested rides for the on-demand system. 8,000 vehicles in the door-to-door system and 5,000 vehicles in the stop-based system are necessary to serve all requests. Similar to the draconian scenario, a small share of requests cannot be served within the given service parameters and is rejected. The ride-pooling kilometers are lower, as fewer rides are served. The total VKT in the service area, however, increases to 10.7 million km for the door-to-door system and to 10.1 million km for the stop-based system. This increase compared to the base case (9.8 million km) is due to an increased number of trips conducted on the road network as the ride-pooling system not only attracts private car users but also agents that used transit, walked or biked before. The share of empty VKT is with 5% and 6% slightly lower than in the draconian scenario. As a consequence of the higher traffic volumes, travel times are noticeable higher in the laissez-faire scenario with 17:01 min and 15:41 min, confirming hypothesis c). Customers also face slightly longer detours.

Computation times per iteration are highly influenced by the number of ride-pooling rides and vehicles. While in the base case, it only takes half an hour to simulate one iteration, the simulation of the draconian door-to-door system takes roughly 24 h. The number of necessary iterations however increases with the number of car trips. To reach a system equilibrium, we simulated 300 iterations for the base case, 4 iterations for both draconian scenarios and 10 iterations for both laissez-faire scenarios.

Fig. 3 shows average waiting times per zone for the two ride-pooling systems in the draconian scenario. The waiting times for the door-to-door service predominantly vary between 4 and 7 min. Waiting times are slightly higher in the city center where request density is highest and consequently vehicle flow volume increases and causes some congestion in peak times. However, the negative effect on the customer side is rather small. At the border of the service area a high variance of average waiting times can be observed. The number of rides starting in some of the outer cells is very small which causes a higher variance. Additionally, we observe a cluster of cells in the north-western part of the service area with higher waiting times. In this area many rides occur due to an industrial zone with many working places and the location next to a street with incoming and outgoing car traffic that is replaced by the ride-pooling

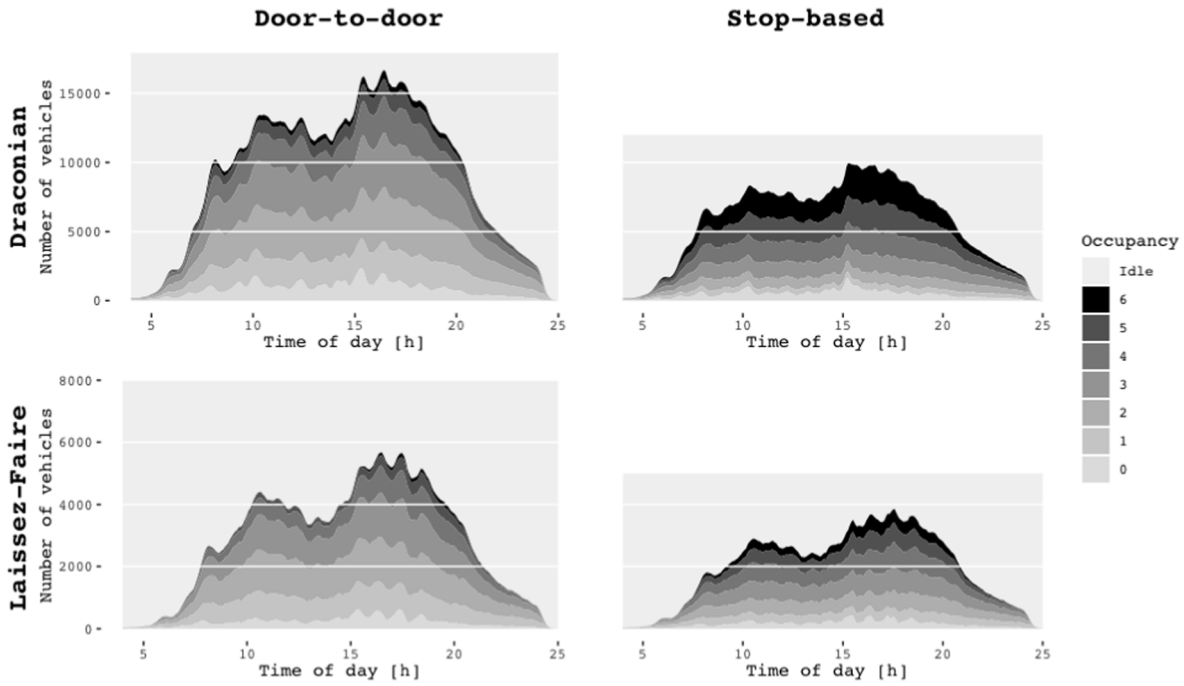

Fig. 4. Vehicle occupancy for the door-to-door (left) and the stop-based (right) service in the draconian (top) and laissez-faire (bottom) ride-pooling scenario.

system. The waiting times for the stop-based service vary between 4 and 6 min and spread evenly across the service area. As the average waiting times are similar across both draconian scenarios and do not vary drastically across the service area, we decided to assume an average waiting time of 5 min for all ride-pooling trips to calculate possible ride-pooling shares in the laissez-faire scenario. As stated earlier, the waiting times are part of the generalized costs.

Fig. 4 shows the vehicle occupancy over time for the two ride-pooling services in both mode choice scenarios. In the draconian scenario the door-to-door service carries six passengers during 4% of the covered distance while the stop-based service carries the maximum number of passenger during 25% of the overall distance, indicating that even larger vehicles than six-seaters could add efficiency.

The occupancy of the vehicle fleet in the laissez-faire scenario indicates a generally lower occupancy compared to the draconian scenario. The door-to-door fleet only carries six passengers during 1% of the distance whereas the stop-based fleet is fully occupied during 10% of the total distance. The lower occupancies in the laissez-faire scenarios are caused by a lower request density, lower travel speeds and fewer detour possibilities due to congested roads. Additionally, all incoming and outgoing traffic in the draconian scenario starts or ends at a street accessing the service area from outside, which leads to a bundling of requests at those peripheral locations.

5.2. Noise analysis

Fig. 5 shows the base scenario noise immissions for all receiver points within the service area. High noise values are observed near major roads, while residential areas show noticeable lower noise levels. Overall, immissions are comparatively high, with about half of urban dwellings experiencing an immission that exceeds 55 dB(A).

The spatial distribution of differences in noise immissions in the ride-pooling scenarios compared to the base case is shown in Fig. 6. The results in the maps shown here do not include the electric correction term.

Noise levels –on average– are nearly the same in the base scenario and in the draconian scenario with a door-to-door service. However, when looking at the spatial distribution of differences, we find that major reductions of noise are estimated along major roads. Pooling rates along major roads are high and traffic volumes are reduced. However, our simulation results show that those reductions are almost fully compensated by increased noise in residential neighborhoods. This can be explained by detours and additional kilometers driven near individual departure/arrival locations to pick up or drop off customers. In addition, pooling rates around pick-up/drop-off points in residential areas tend to be lower than at major connecting roads. The logarithmic dose–response

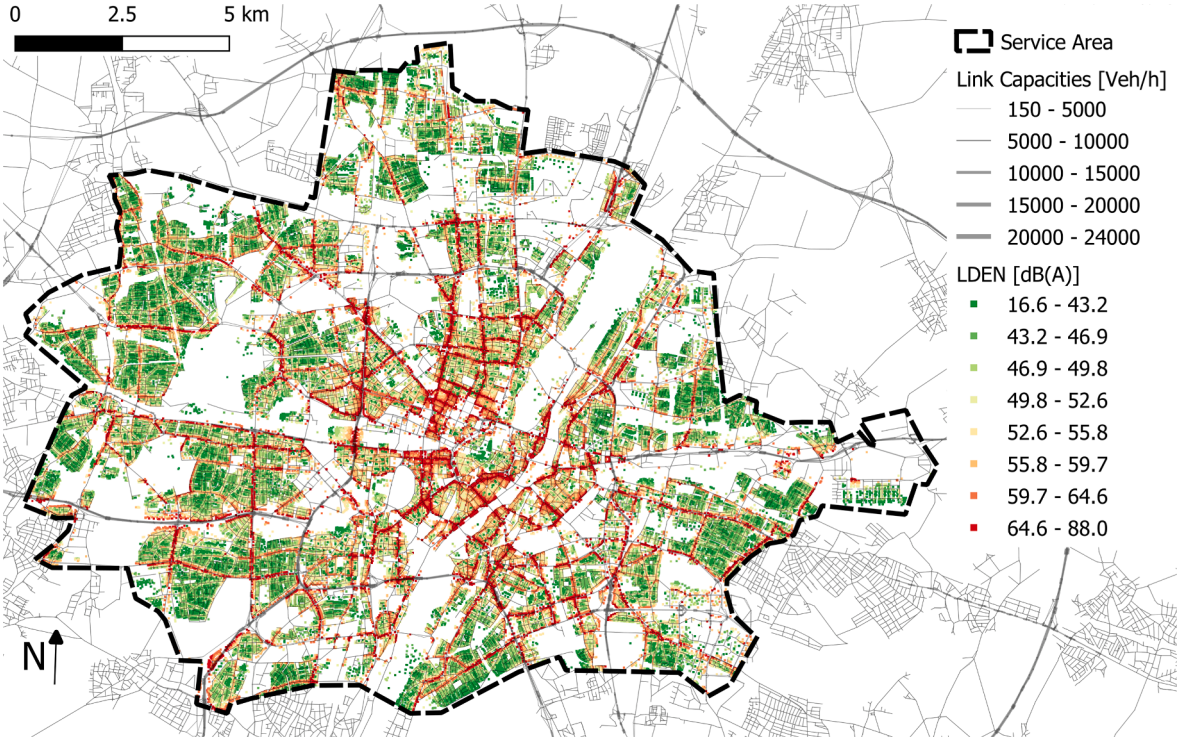

Fig. 5. Base scenario noise exposure in the given service area in Munich. L_{DEN} values presented in quantile ranges.

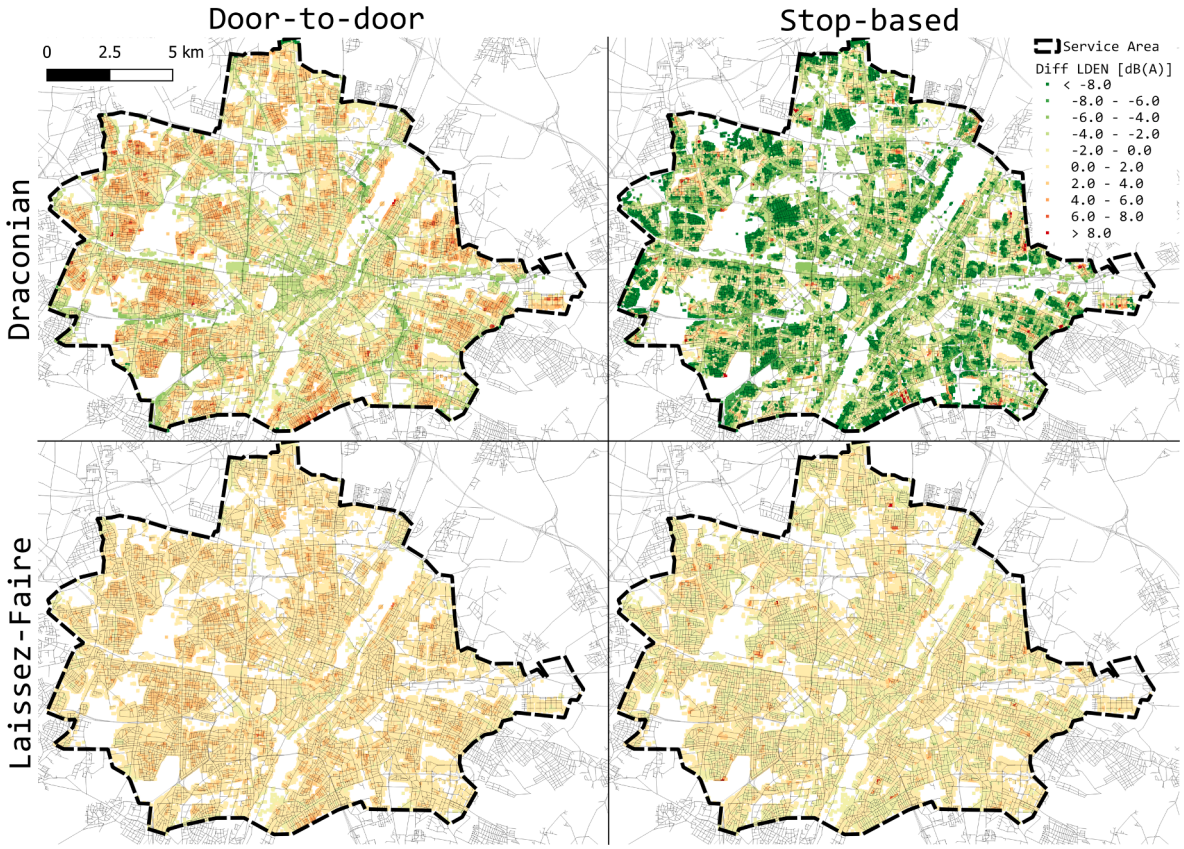

Fig. 6. Difference in L_{DEN} values for the door-to-door (left) and the stop-based (right) service in the draconian (top) and laissez-faire (bottom) ride-pooling scenario when compared to the base scenario immission values for dwellings inside the study area. Green values indicate a reduction of noise compared to the base case. Red values represent an increase.

relationship between traffic volume and noise leads to relatively high increases in noise at residential areas, where traffic volumes are low and small changes in volume lead to high changes in noise. More consistent reductions in noise can be seen with the stop-based service, due to multiple reasons. First, fewer vehicles are required as the pooling rate is higher, leading overall to lower traffic volumes. Secondly, a few hundred meters of the trips are done by walking and lastly, quite a few links do not experience any traffic at all since vehicles only route between stops. This –in contrast to a door-to-door service– leads to some very quiet residential roads and

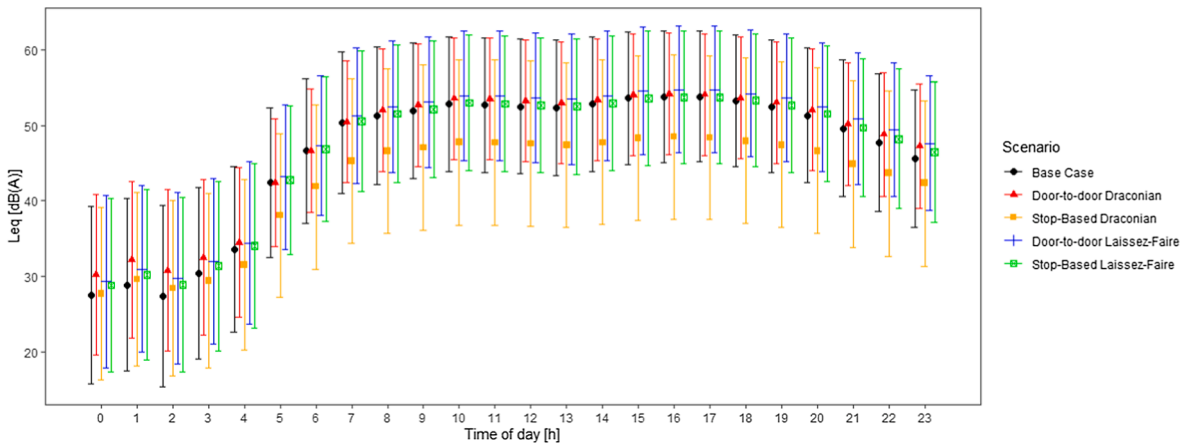

Fig. 7. Hourly equivalent sound levels L_{eq} across 24 h for each scenario. Symbols represent the mean across all receiver points, bars delimit standard deviations.

neighborhoods. A few selected sites still experience an increase in noise. These are mostly near stops where traffic volumes can be higher.

The impacts on noise are generally smaller in the laissez-faire scenario, which is driven by the fact that the fleet sizes are smaller and private car traffic remains a main source of traffic noise. Again, the door-to-door service leads to more noise than the stop-based service. However, since the overall traffic volumes increase in many places, there is almost no compensation at larger roads. With the stop-based service, changes in noise exposure are very small and happen in either direction with no distinct spatial pattern. This is remarkable in that 53% of the additional ride-pooling passengers previously used one of the modes *walk*, *bike* or *public transport* and are now additionally riding on the road network.

Fig. 7 shows the temporal variations of the hourly equivalent sound level L_{eq} for each scenario. In general, the variation between scenarios is higher in the morning hours, where traffic volumes are typically low and changes in volume are reflected by higher changes in noise. During the day, the mean hourly sound levels stay very similar across all scenarios, except the draconian stop-based scenario. Here, the mean L_{eq} is constantly significantly lower than in the other scenarios. This indicates that the reduction in noise is stable across the day.

The gap between the last and the first hour of the day is a typical limitation of transport models that run for one day only. However, because of its logarithmic nature (see Eq. 2), the L_{DEN} indicator is mostly driven by the maximum levels across a day and therefore robust against inaccuracies in lower noise levels that occur at night.

Table 4 shows a comparison of descriptive statistics while Fig. 8 shows the overall distributions of L_{DEN} values in the different scenarios and the base case. Note that we also show the results for the draconian scenario with the electric correction term. In the laissez-faire scenario, the correction term did not lead to any noteworthy changes. The depicted threshold of 55 dB(A) was chosen as the target threshold defined by the European Union (2002).

In the laissez-faire scenario, mean noise immissions increased slightly. While the overall distribution with a stop-based service looks similar to the base case distribution, a door-to-door service increases the share of highly exposed dwellings by around 5%. In the draconian scenario with door-to-door service, the mean immission value is slightly higher than in the base case, although VKT in the service area are reduced by 33%. However, when looking at the distribution and standard error, it shows that the immissions are distributed more evenly across all dwellings. Nonetheless, the share of highly exposed dwellings increases by 3%. The draconian scenario with a stop-based ride-pooling service including the correction term for electric vehicles shows the highest reductions in noise, with a mean L_{DEN} of 48.41 dB(A) and only 30% of the dwellings being exposed to more than 55 dB(A). The stop-based service here leads to higher standard errors and less equally distributed immissions (compare "quiet" residential neighborhoods in Fig. 6). Under the given assumptions, reductions in noise can be quite significant when a correction is considered for electric vehicles. However, our results suggest that these only become visible once a major share of the vehicles on the road is electric.

Fig. 9 shows the density distribution of differences in L_{DEN} values. While the overall distribution in Fig. 8 suggests that, in the draconian door-to-door scenario, the distribution did not change systematically apart from a slight increase, the distribution of differences reveals that noise levels indeed change. However, in line with the spatial distribution in Fig. 6, changes happen in both directions and therefore "compensate" to some degree. The draconian stop-based scenarios show a clear trend towards reduced noise levels while the laissez-faire scenarios barely expose any noteworthy differences. The electric correction term seems to maintain the shape of the distribution while pushing it more towards reduced noise levels.

Overall, it can be seen that a reduction of noise can be accomplished by a stop-based ride-pooling service in a draconian scenario. The door-to-door service tends to increase noise in residential areas, where most people live and where traffic increases because of pick-up and drop-off rides. In general, traffic noise is mainly moderated through traffic volumes and speeds (see Fig. 1). Consequently, hypothesis a) only holds true for the stop-based service in which traffic volumes decreased thoroughly whereas for the door-to-door service traffic volumes only decreased on major streets.

In the laissez-faire scenario, a stop-based service can keep noise at similar levels as in the base case, even though the amount of road trips increases. Because of the logarithmic dose–response-relationship between traffic volume and noise, the impacts on the aggregated L_{DEN} value is small compared to the changes in traffic volumes and VKT. The results confirm hypothesis b) as residential noise exposure is generally further decreased with a stop-based service than with a door-to-door service.

Table 4
Descriptive statistics of noise immission results.

	Base case	Draconian scenario				Laissez-faire scenario	
		Door-to-door	Door-to-door electric	Stop-based	Stop-based electric	Door-to-door	Stop-based
Mean L_{DEN} [dB]	53.17	53.68	51.93	48.41	46.92	54.29	53.37
Median L_{DEN} [dB]	52.57	53.77	51.83	48.31	46.72	54.00	52.85
Min L_{DEN} [dB]	16.64	15.51	13.825	2.75	2.52	16.95	17.04
Max L_{DEN} [dB]	87.99	84.68	83.77	83.84	82.94	88.39	88.37
S.E. L_{DEN} [dB]	8.89	8.04	8.17	10.78	10.82	8.60	8.96
Share >55 dB [%]	40	43	34	30	26	45	41

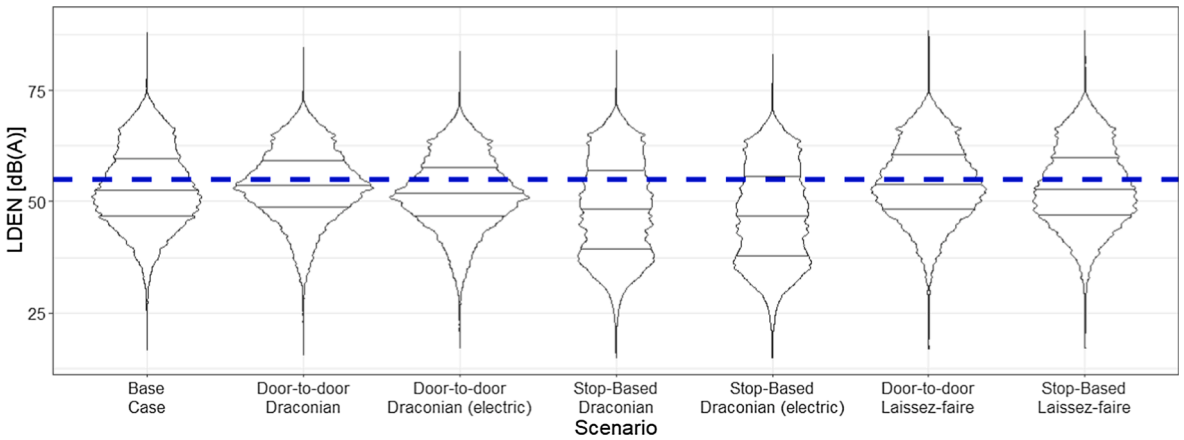

Fig. 8. Violin plots with quantiles for the distribution of L_{DEN} values of dwellings in the presented scenarios. The dashed line depicts the threshold value of 55 dB(A).

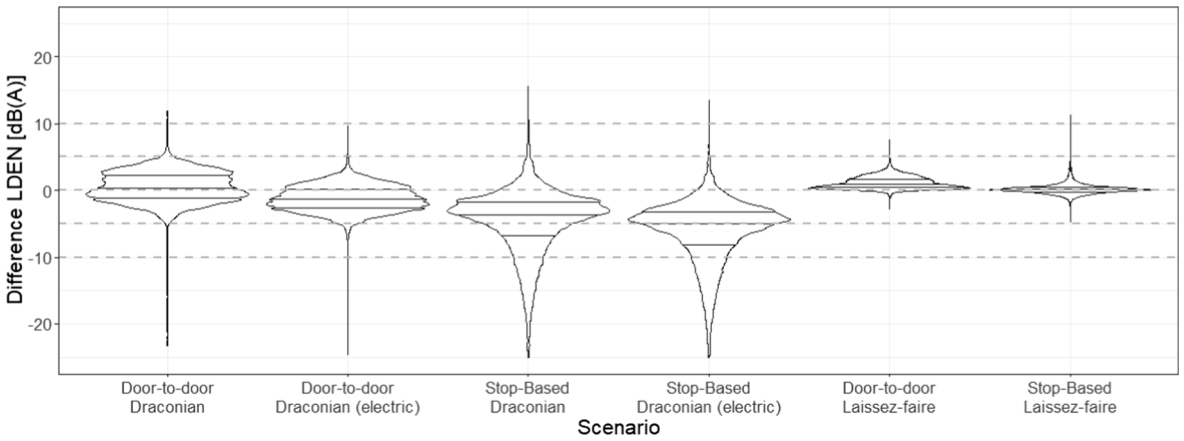

Fig. 9. Violin plots with quantiles for the distribution of *differences* of L_{DEN} values of dwellings as compared to the base case.

6. Discussion and conclusion

The proposed ride-pooling scenarios show the influence of different mode choice settings and service designs on a large scale. We used a state of the art ride-pooling strategy and assessed the impacts with an updated noise prediction model in MATSim. However, we identified some limitations of the investigation.

A limitation for the laissez-faire scenario is that it is difficult to estimate reasonable mode shares for the ride-pooling system. As observed ride-pooling data are not available for Munich, one could re-estimate a mode choice model with automated ride-pooling based on stated preference data. However, since most of the current services are relatively new and not autonomous, a survey may only include hypothetical mode choice options. More reliable estimates could be derived by using estimated value of times (VOT) for pooled rides to have a better idea of the impacts of (generalized) costs (see e.g. Alonso-González et al. (2020)). Instead of doing the mode choice in MITO, the mode choice could be included in MATSim, enabling the consideration of the actual experienced service levels for each agent. However, since the simulation of ride-pooling with a 100% sample runs up to 24 h per iteration, adding mode choice would require several weeks to run the model, as many more iterations are required to reach an equilibrium. This could be reduced partly by using a discrete mode choice model instead of random mutations in MATSim as described in Hörl et al. (2018). The advantage of simulating mode choice in MATSim would be the feedback loop from actual travel times to the decision making throughout iterations. But even then, utility parameters would be hypothetical.

Another limitation is that both scenarios do not account for induced demand, as the trip generation phase in MITO is not affected by the availability of the ride-pooling system. In reality, however, it could happen that people do additional trips once cheap automated ride-pooling trips become available, as observed by Henao and Marshall (2019) for ride-hailing. This could be especially true for otherwise less mobile persons, i.e. persons without cars/drivers' license, children, persons with disabilities or elderly people.

The two scenarios presented in this study show possible outcomes under a set of assumptions and after the service is completely introduced/enforced. As pointed out in Basu and Ferreira (2020), it should be acknowledged that exogenous assumptions and the complete replacement assumption limit the use of studies like ours to the identification of long-term possibilities of new technologies. The authors stress the importance of market dynamics, which can impact acceptance and regulations. Haboucha et al. (2017) presented a stated preference study and find quite a reluctance to use shared autonomous vehicles (which were not even defined as a pooled service and just as a replacement to a privately owned vehicle), with 25% of respondents stating unwillingness to use shared autonomous vehicles even if the service was free. In addition, respondents would rather not use the autonomous service to send children to school, which indicated safety reservations towards automated services. Parents would probably be even more cautious if they had to decide to use a shared service that is pooled with strangers.

While the detours and empty-kilometers of ride-pooling vehicles can lead to increased noise levels in residential areas, the present study does not account for the challenge of parking search for car traffic. A preceding study that included parking search in the simulation found that traffic volumes can be increased by up to 20% in residential areas when parking search is included (Bischoff and Nagel, 2017). As parking search only applies to personally owned vehicles and not to pooled vehicles, the differences in noise levels between the base scenario and the ride-pooling scenarios would be even more pronounced.

We ignore commercial vehicles, which can significantly contribute to noise emission. The conclusions of this research, however, are likely to hold true. The main limitation can be found on major roads where most commercial vehicle traffic contributes to noise. The impact of these scenarios is expected to be slightly smaller once noise from commercial vehicles is added to the analysis.

The chosen correction term for electric vehicles may reflect noise reductions reasonably well for the applicable speed range of the implemented noise guideline. However, higher reductions should emerge at intersections where acceleration noises of engines make up a large share of the resulting noise immission. Therefore, we assume that we broadly underestimate possible noise reductions at intersections, since acceleration is not modeled in MATSim and the guideline assumes a minimum speed of 30 km/h. This underestimation could be alleviated if EVs are required to be equipped with an acoustic alerting system at low speeds.

Another limitation is that we implement one single operator which only offers pooled rides. Ruch et al. (2020) showed that it is unclear if the efficiency gains of ride-pooling compensate for the loss of privacy and a lower service level compared to an unpooled system. Private operators may generate higher revenues by offering private rides, which would again lead to more VKT and noise exposure. Thus, from a macroeconomic point of view, it could be beneficial for policy makers to incentivise the supply of pooled on-demand services compared to unpooled services.

Given the current limitations, the present study shows remarkable results that can be generalized. It is shown that the implementation of an efficient ride-pooling system requires a well-elaborated strategy. The draconian scenario shows the high potential of ride-pooling to serve the same demand with less resources than the current car system. Assuming that each private vehicle in the service area is on average used for 3 rides per day, more than 600,000 private vehicles are necessary to transport the same amount of rides as 12,000 stop-based ride-pooling vehicles. According to that, one ride-pooling vehicle could replace more than 50 private vehicles. In addition, major noise reductions can be achieved with a draconian replacement of all private vehicles with electric pooled vehicles and a stop-based service. Although VKT are also reduced with a door-to-door service, average noise exposure increases since more traffic occurs in residential areas. The laissez-faire scenarios indicate that only by implementing the new service, road traffic does not decrease as agents that previously chose other modes than *car* are attracted. A stop-based system is again more efficient than the door-to-door service. To meet all travel needs of current car users, it may be beneficial to implement a mixed service that offers a stop-based option and a door-to-door option at a higher price level. The implementation of a mixed service including the mode choice might be subject of further research as well as the investigation of different pooling strategies in combination with additional public policies.

Declaration of interests

Felix Zwick is currently a PhD candidate at ETH Zurich and scientifically studies the impacts of ridepooling. However, it is also acknowledged that he is employed at the ride-pooling provider MOIA.

CRediT authorship contribution statement

Felix Zwick: Conceptualization, Methodology, Software, Validation, Formal analysis, Investigation, Resources, Data curation, Writing - original draft, Visualization. **Nico Kuehnel:** Conceptualization, Methodology, Software, Validation, Formal analysis, Investigation, Resources, Data curation, Writing - original draft, Visualization. **Rolf Moeckel:** Conceptualization, Writing - review & editing, Supervision. **Kay W. Axhausen:** Conceptualization, Writing - review & editing, Supervision.

Appendix A

We start from Eq. (8):

$$L_{\mathrm{W},j_i,k,t}(v_{j_i,k,t}) = L_{\mathrm{W0},k,t}(v_{j_i,k,t}) + D_{\mathrm{surf}_{j_i},k}(v_{j_i,k,t}) + D_{\mathrm{grad}_{j_i},k}(g_{j_i}, v_{j_i,k,t}) + D_{\mathrm{inter}}(x_{j_i}) + D_{\mathrm{electric}}(v_{j_i,k,t})$$

We assume that velocity, surface and gradient stay constant across all segments j_i of a link i:

$$\begin{aligned} v_{j_i,k,t} &\overset{\text{def}}{=} v_{i,k,t}, \quad \forall j_i \in i, \forall i \\ D_{\text{surf}_{j_i},k}(v_{j_i,k,t}) &\overset{\text{def}}{=} D_{\text{surf}_i,k}(v_{i,k,t}), \quad \forall j_i \in i, \forall i \\ D_{\text{grad}_{j_i},k}(g_{j_i}, v_{j_i,k,t}) &\overset{\text{def}}{=} D_{\text{grad}_i,k}(g_i, v_{i,k,t}), \quad \forall j_i \in i, \forall i \end{aligned}$$

Now only the intersection term $D_{\text{inter}}(x_{j_i})$ still depends on the actual segment. We separate the intersection term and define:

$$\begin{aligned} &L_{\text{W},j_i,k,t}(v_{i,k,t}) = L_{\text{W},i,k,t}(v_{i,k,t}) + D_{\text{inter}}(x_{j_i}), \text{ with} \\ &L_{\text{W},i,k,t}(v_{i,k,t}) = L_{\text{W0},k,t}(v_{i,k,t}) + D_{\text{surf},k}(v_{i,k,t}) + D_{\text{grad},k}(g, v_{i,k,t}) + D_{\text{electric}}(v_{i,k,t}) \end{aligned}$$

Using this, we update Eq. (4):

$$L_{\text{W},j_i,t} = 10 \cdot \log_{10}[M_{j_i,t}] + 10 \cdot \log_{10}\left[\sum_k \lambda_{j_i,k,t} \cdot \frac{10^{0.1 \cdot (L_{\text{W},i,k,t}(v_{k,t}) + D_{\text{inter}}(x_{j_i}))}}{v_{i,k,t}}\right] - 30$$

$$L_{\text{W},j_i,t} = 10 \cdot \log_{10}[M_{j_i,t}] + 10 \cdot \log_{10}\left[\sum_k \lambda_{j_i,k,t} \cdot \frac{10^{0.1 \cdot L_{\text{W},i,k,t}(v_{i,k,t}) + 0.1 \cdot D_{\text{inter}}(x_{j_i})}}{v_{i,k,t}}\right] - 30$$

$$L_{\text{W},j_i,t} = 10 \cdot \log_{10}[M_{j_i,t}] + 10 \cdot \log_{10}\left[\sum_k \lambda_{j_i,k,t} \cdot \frac{10^{0.1 \cdot L_{\text{W},i,k,t}(v_{i,k,t})} \cdot 10^{0.1 \cdot D_{\text{inter}}(x_{j_i})}}{v_{i,k,t}}\right] - 30$$

$$L_{\text{W},j_i,t} = 10 \cdot \log_{10}[M_{j_i,t}] + 10 \cdot \log_{10}\left[10^{0.1 \cdot D_{\text{inter}}(x_{j_i})} \cdot \sum_k \lambda_{j_i,k,t} \cdot \frac{10^{0.1 \cdot L_{\text{W},i,k,t}(v_{k,t})}}{v_{i,k,t}}\right] - 30$$

$$L_{\text{W},j_i,t} = 10 \cdot \log_{10}[M_{j_i,t}] + 10 \cdot \left\{\log_{10}\left[10^{0.1 \cdot D_{\text{inter}}(x_{j_i})}\right] + \log_{10}\left[\sum_k \lambda_{j_i,k,t} \cdot \frac{10^{0.1 \cdot L_{\text{W},i,k,t}(v_{k,t})}}{v_{i,k,t}}\right]\right\} - 30$$

$$L_{\text{W},j_i,t} = 10 \cdot \log_{10}[M_{j_i,t}] + D_{\text{inter}}(x_{j_i}) + 10 \cdot \log_{10}\left[\sum_k \lambda_{j_i,k,t} \cdot \frac{10^{0.1 \cdot L_{\text{W},i,k,t}(v_{k,t})}}{v_{i,k,t}}\right] - 30$$

Next, we also assume that traffic volumes M_{j_i}, and vehicle type shares λ_{j_i} stay constant across all segments j_i of a link i:

$$\begin{aligned} M_{j_i} &\overset{\text{def}}{=} M_i, \quad \forall j_i \in i, \forall i \\ \lambda_{j_i} &\overset{\text{def}}{=} \lambda_i, \quad \forall j_i \in i, \forall i \end{aligned}$$

Now we can separate the segment-dependent intersection term again:

$$\begin{aligned} &L_{\text{W},j_i,t} = L_{\text{W},i,t} + D_{\text{inter}}(x_{j_i}), \text{ with} \\ &L_{\text{W},i,t} = L_{\text{W0},k,t}(v_{k,t}) + 10 \cdot \log_{10}[M_{i,t}] + 10 \cdot \log_{10}\left[\sum_k \lambda_{i,k,t} \cdot \frac{10^{0.1 \cdot L_{\text{W},i,k,t}(v_{k,t})}}{v_{i,k,t}}\right] - 30 \end{aligned}$$

We can now update the immission calculation shown in Eq. (3):

$$L_{\text{eq},k,t} = 10 \cdot \log_{10} \sum_i \sum_{j_i} 10^{0.1 \cdot (L_{\text{W},i,t} + D_{\text{inter}}(x_{j_i}) + 10 \cdot \log_{10}[l_{j_i}] - D_{\text{A},j_i} - D_{\text{RV1},j_i} - D_{\text{RV2},j_i})}$$

We ignore the impact of reflections in our approach and set $D_{\text{RV1},j_i} = D_{\text{RV2},j_i} \overset{\text{def}}{=} 0$. We now separate time- from segment-dependent terms:

$$L_{\text{eq},k,t} = 10 \cdot \log_{10}\left[\sum_i \sum_{j_i} 10^{0.1 \cdot (L_{\text{W},i,t} + D_{\text{inter}}(x_{j_i}) + 10 \cdot \log_{10}[l_{j_i}] - D_{\text{A},j_i})}\right]$$

$$L_{\text{eq},k,t} = 10 \cdot \log_{10}\left[\sum_i \sum_{j_i} 10^{0.1 \cdot L_{\text{W},i,t} + 0.1 \cdot (D_{\text{inter}}(x_{j_i}) + 10 \cdot \log_{10}[l_{j_i}] - D_{\text{A},j_i})}\right]$$

$$L_{\text{eq},k,t} = 10 \cdot \log_{10}\left[\sum_i \sum_{j_i} 10^{0.1 \cdot L_{\text{W},i,t}} \cdot 10^{0.1 \cdot (D_{\text{inter}}(x_{j_i}) + 10 \cdot \log_{10}[l_{j_i}] - D_{\text{A},j_i})}\right]$$

$$L_{\text{eq},k,t} = 10 \cdot \log_{10}\left[\sum_i 10^{0.1 \cdot L_{\text{W},i,t}} \cdot \sum_{j_i} 10^{0.1 \cdot (D_{\text{inter}}(x_{j_i}) + 10 \cdot \log_{10}[l_{j_i}] - D_{\text{A},j_i})}\right]$$

Now, only the first part of the equation depends on t. The second part basically sums up all correction terms for the respective link segments and can be summarized as c_i :

$$L_{\mathrm{eq},k,t} = 10 \cdot \log_{10}\left[\sum_i \left(10^{0.1 \cdot L_{\mathrm{W},i,t}} \cdot c_i\right)\right], \text{ with}$$
$$c_i = \sum_{j_i} 10^{0.1 \cdot (D_{\mathrm{inter}}(x_{j_i}) + 10 \cdot \log_{10}[l_{j_i}] - D_{\mathrm{A},j_i})}$$

References

(2002). Directive 2002/49/EC of the European Parliament and of the Council of 25 June 2002 relating to the assessment and management of environmental noise - Declaration by the Commission in the Conciliation Committee on the Directive relating to the assessment a. Off. J. L 189, 0012–0026.

Alonso-González, M.J., [van Oort], N., Cats, O., Hoogendoorn-Lanser, S., Hoogendoorn, S., 2020. Value of time and reliability for urban pooled on-demand services. Transport. Res. Part C: Emerg. Technol. 115, 102621.

Alonso-Mora, J., Samaranayake, S., Wallar, A., Frazzoli, E., Rus, D., 2017. On-demand high-capacity ride-sharing via dynamic trip-vehicle assignment. Proc. Nat. Acad. Sci. USA 114 (3), 462–467.

Basu, R., Ferreira, J., 2020. A LUTI microsimulation framework to evaluate long-term impacts of automated mobility on the choice of housing-mobility bundles. Environ. Plann. B: Urban Anal. City Sci. 239980832092527.

Bekke, D., Wijnant, Y., Weegerink, T., De Boer, A., 2013. Tire-road noise: An experimental study of tire and road design parameters. In: 42nd International Congress and Exposition on Noise Control Engineering 2013, INTER-NOISE 2013: Noise Control for Quality of Life, vol. 1, pp. 173–180.

Bischoff, J., Kaddoura, I., Maciejewski, M., Nagel, K., 2018. Simulation-based optimization of service areas for pooled ride-hailing operators. Procedia Comput. Sci. 130, 816–823.

Bischoff, J., Maciejewski, M., 2016. Simulation of city-wide replacement of private cars with autonomous Taxis in Berlin. Procedia Comput. Sci. 83, 237–244.

Bischoff, J., Maciejewski, M., 2020. Proactive empty vehicle rebalancing for Demand Responsive Transport services. Procedia Comput. Sci. 170, 739–744.

Bischoff, J., Maciejewski, M., Nagel, K., 2017. City-wide shared taxis: A simulation study in Berlin. In: IEEE Conference on Intelligent Transportation Systems, Proceedings, ITSC.

Bischoff, J., Nagel, K., 2017. Integrating explicit parking search into a transport simulation. Procedia Comput. Sci., 109, 881–886. 8th International Conference on Ambient Systems, Networks and Technologies, ANT-2017 and the 7th International Conference on Sustainable Energy Information Technology, SEIT 2017, 16-19 May 2017, Madeira, Portugal.

Bradley, J.S., Jonah, B.A., 1979. The effects of site selected variables on human responses to traffic noise, Part II: Road type by socio-economic status by traffic noise level. J. Sound Vib. 67 (3), 395–407.

Brown, A.L., Van Kamp, I., 2017. Who environmental noise guidelines for the european region: A systematic review of transport noise interventions and their impacts on health. Int. J. Environ. Res. Public Health 14 (8).

Bösch, P.M., Becker, F., Becker, H., Axhausen, K.W., 2018. Cost-based analysis of autonomous mobility services. Transp. Policy 64, 76–91.

Campello-Vicente, H., Peral-Orts, R., Campillo-Davo, N., Velasco-Sanchez, E., 2017. The effect of electric vehicles on urban noise maps. Appl. Acoust. 116, 59–64.

Clark, C., Paunovic, K., 2018. Who environmental noise guidelines for the european region: A systematic review on environmental noise and quality of life, wellbeing and mental health. Int. J. Environ. Res. Public Health 15 (11).

CleverShuttle, 2020. https://www.clevershuttle.de/. Last accessed: 2020-08-19.

Engelhardt, R., Dandl, F., Bilali, A., Bogenberger, K., 2019. Quantifying the benefits of autonomous on-demand ride-pooling: a simulation study for Munich, Germany. In: 2019 IEEE Intelligent Transportation Systems Conference (ITSC). IEEE, pp. 2992–2997.

European Environment Agency, 2018. Environmental indicator report 2018. https://www.eea.europa.eu/airs/2018.

Fagnant, D.J., Kockelman, K.M., 2018. Dynamic ride-sharing and fleet sizing for a system of shared autonomous vehicles in Austin. Texas. Transport. 45 (1), 143–158.

FGSV, 1990. Richtlinien für den Lärmschutz an Straßen (RLS). Technical report.

FGSV, 2019. Richtlinien für den Lärmschutz an Straßen (RLS). Technical report.

Forbes, 2008. In depth: Europe's most congested cities. https://www.forbes.com/2008/04/21/europe-commute-congestion-forbeslife-cx_po_0421congestion_slide.html. Last accessed: 2020-08-12.

Garg, N., Maji, S., 2014. A critical review of principal traffic noise models: Strategies and implications. Environ. Impact Assess. Rev. 46, 68–81.

GrabShare, 2020. https://www.grab.com/ph/transport/share/. Last accessed: 2020-07-29.

Greenblatt, J.B., Saxena, S., 2015. Autonomous taxis could greatly reduce greenhouse-gas emissions of US light-duty vehicles. Nature Climate Change 5 (9), 860–863.

Gurumurthy, K.M., Kockelman, K.M., 2020. How much does greater trip demand and aggregation at stops improve dynamic ride-sharing in shared autonomous vehicle systems? Preprint at https://www.researchgate.net/publication/343451580.

Guski, R., Schreckenberg, D., Schuemer, R., 2017. Who environmental noise guidelines for the european region: A systematic review on environmental noise and annoyance. Int. J. Environ. Res. Public Health 14 (12).

Haboucha, C.J., Ishaq, R., Shiftan, Y., 2017. User preferences regarding autonomous vehicles. Transport. Res. Part C: Emerg. Technol. 78, 37–49.

Henao, A., Marshall, W.E., 2019. The impact of ride-hailing on vehicle miles traveled. Transportation 46 (6), 2173–2194.

Hörl, S., 2017. Agent-based simulation of autonomous taxi services with dynamic demand responses. Procedia Comput. Sci. 109, 899–904.

Hörl, S., Balac, M., Axhausen, K.W., 2018. A first look at bridging discrete choice modeling and agent-based microsimulation in MATSim. In: Procedia Computer Science, vol. 130. Elsevier B.V., pp. 900–907.

Horni, A., Nagel, K., Axhausen, K.W. (Eds.), 2016. The Multi-Agent Transport Simulation MATSim. Ubiquity Press, London.

Infas and DLR, 2010. Mobilität in Deutschland 2008. Technical report, infas Institut für angewandte Sozialwissenschaft GmbH and Deutschles Zentrum für Luft- und Raumfahrt e.v., Bonn and Berlin.

Iversen, L.M., Marbjerg, G., Bendtsen, H., 2013. Noise from electric vehicles-'state-of-the-art' literature survey. In inter-noise, Innsbruck.

Jabben, J., Verheijen, E., Potma, C., 2012. Noise reduction by electric vehicles in the Netherlands. In: INTER-NOISE and NOISE-CON Congress and Conference Proceedings, vol. 2012. Institute of Noise Control Engineering, pp. 6958–6965.

Jing, P., Hu, H., Zhan, F., Chen, Y., Shi, Y., 2020. Agent-based simulation of autonomous vehicles: a systematic literature review. IEEE Access 8, 79089–79103.

Kaddoura, I., Kröger, L., Nagel, K., 2017. An activity-based and dynamic approach to calculate road traffic noise damages. Transport. Res. Part D: Transport Environ. 54, 335–347.

Koppelman, F.S., 1983. Predicting transit ridership in response to transit service changes. J. Transport. Eng. 109 (4), 548–564.

Kuehnel, N., Kaddoura, I., Moeckel, R., 2019. Noise shielding in an agent-based transport model using volunteered geographic data. In: Procedia Computer Science, vol. 151. Elsevier, pp. 808–813.

Kuehnel, N., Moeckel, R., 2020. Impact of simulation-based traffic noise on rent prices. Transport. Res. Part D: Transport Environ. 78, 102191.

Leich, G., Bischoff, J., 2019. Should autonomous shared taxis replace buses? A simulation study. Transport. Res. Procedia 41, 450–460.

Ma, S., Zheng, Y., Wolfson, O. 2013. T-share: A large-scale dynamic taxi ridesharing service. In: Proceedings - International Conference on Data Engineering, pp. 410–421.

Maciejewski, M., 2016. Dynamic Transport Services. In: Andreas Horni, Kai Nagel, Axhausen Kay W. (Eds.), The Multi-Agent Transport Simulation MATSim, pp. 145–152 (chapter 23).
Martinez, L.M., Viegas, J.M., 2017. Assessing the impacts of deploying a shared self-driving urban mobility system: An agent-based model applied to the city of Lisbon, Portugal. Int. J. Transport. Sci. Technol. 6 (1), 13–27.
Moeckel, R., Kuehnel, N., Llorca, C., Moreno, A.T., Rayaprolu, H., 2020. Agent-based simulation to improve policy sensitivity of trip-based models. J. Adv. Transport. 2020, 1902162.
MOIA, 2020. https://www.moia.io/. Last accessed: 2020-08-19.
Moreno, A., Moeckel, R., 2018. Population synthesis handling three geographical resolutions. ISPRS Int. J. Geo-Informat. 7 (5), 174.
OpenStreetMap Contributors, 2018. OpenStreetMap. www.openstreetmap.org. Last accessed: 2018-07-26.
Naumov, Sergey, Keith, David R., Fine, Charles H., 2020. Unintended Consequences of Automated Vehicles and Pooling for Urban Transportation Systems. Production and Operations Management 29 (5), 1354–1371. https://doi.org/10.1111/poms.13166.
Osada, Y., Yoshida, T., Yoshida, K., Kawaguchi, T., Hoshiyama, Y., Yamamoto, K., 1997. Path analysis of the community response to road traffic noise. J. Sound Vib. 205 (4), 493–498.
Pernestål, A., Kristoffersson, I., 2019. Effects of driverless vehicles: Comparing simulations to get a broader picture. Eur. J. Transport Infrastruct. Res. 1 (19), 1–23.
Quartieri, J., Iannone, G., Guarnaccia, C., D'Ambrosio, S., Troisi, A., Lenza, T., 2009. A review of traffic noise predictive models. In: Recent Advances in Applied and Theoretical Mechanics.
Ruch, C., Horl, S., Frazzoli, E., 2018. AMoDeus, a simulation-based testbed for autonomous mobility-on-demand systems. In: 2018 21st International Conference on Intelligent Transportation Systems (ITSC), volume 2018-Novem. IEEE, pp. 3639–3644.
Ruch, C., Lu, C., Sieber, L., Frazzoli, E., 2020. Quantifying the efficiency of ride sharing. IEEE Trans. Intell. Transp. Syst. 1–6.
UberPool, 2020. https://www.uber.com/de/en/ride/uberpool/. Last accessed: 2020-07-29.
Verheijen, E., Jabben, J., 2010. Effect of electric cars on traffic noise and safety.
Vosooghi, R., Puchinger, J., Jankovic, M., Vouillon, A., 2019. Shared autonomous vehicle simulation and service design. Transport. Res. Part C: Emerg. Technol. 107, 15–33.
Wang, B., Ordonez Medina, S.A., Fourie, P., 2018. Simulation of autonomous transit on demand for fleet size and deployment strategy optimization. Procedia Comput. Sci. 130, 797–802.
Wardman, M., Bristow, A.L., 2004. Traffic related noise and air quality valuations: Evidence from stated preference residential choice models. Transport. Res. Part D: Transport Environ. 9 (1), 1–27.
WHO, 2009. Night Noise Guidelines for Europe. Technical report. world Health Organization.
Źróbek, S., Trojanek, M., Źróbek-Sokolnik, A., Trojanek, R., 2015. The influence of environmental factors on property buyers' choice of residential location in Poland. J. Int. Stud. 8 (3), 164–174.
Zwick, F., Axhausen, K.W., 2020a. Analysis of ridepooling strategies with MATSim. In: 20th Swiss Transport Research Conference.
Zwick, F., Axhausen, K.W., 2020b. Impact of Service Design on Urban Ridepooling Systems. In: 2020 IEEE Intelligent Transportation Systems Conference (ITSC).